

# Transport methods for probing the barrier domain of lipid bilayer membranes

Tian-xiang Xiang, Xueling Chen, and Bradley D. Anderson

Department of Pharmaceuticals, University of Utah, Salt Lake City, Utah 84112

**ABSTRACT** Two experimental techniques have been utilized to explore the barrier properties of lecithin/decane bilayer membranes with the aim of determining the contributions of various domains within the bilayer to the overall barrier. The thickness of lecithin/decane bilayers was systematically varied by modulating the chemical potential of decane in the annulus surrounding the bilayer using different mole fractions of squalene in decane. The dependence of permeability of a model permeant (acetamide) on the thickness of the solvent-filled region of the bilayer was assessed in these bilayers to determine the contribution of this region to the overall barrier. The flux of acetamide was found to vary linearly with bilayer area with  $P_m = (2.9 \pm 0.3) \times 10^{-4} \text{ cm s}^{-1}$ , after correcting for diffusion through unstirred water layers. The ratio between the overall membrane permeability coefficient and that calculated for diffusion through the hydrocarbon core in membranes having maximum thickness was 0.24, suggesting that the solvent domain contributes only slightly to the overall barrier properties. Consistent with these results, the permeability of acetamide was found to be independent of bilayer thickness.

The relative contributions of the bilayer interface and ordered hydrocarbon regions to the transport barrier may be evaluated qualitatively by exploring the effective chemical nature of the barrier microenvironment. This may be probed by comparing functional group contributions to transport with those obtained for partitioning between water and various model bulk solvents ranging in polarity or hydrogen-bonding potential. A novel approach is described for obtaining group contributions to transport using ionizable permeants and pH adjustment. Using this approach, bilayer permeability coefficients of *p*-toluic acid and *p*-hydroxymethyl benzoic acid were determined to be  $1.1 \pm 0.2 \text{ cm s}^{-1}$  and  $(1.6 \pm 0.4) \times 10^{-3} \text{ cm s}^{-1}$ , respectively. From these values, the  $-\text{OH}$  group contribution to bilayer transport [ $\Delta(\Delta G_{\text{OH}}^0)$ ] was found to be 3.9 kcal/mol. This result suggests that the barrier region of the bilayer does not resemble the hydrogen-bonding environment found in octanol, but is somewhat less selective (more polar) than a hydrocarbon solvent.

## INTRODUCTION

Lipid bilayers are a fundamental component of biological membranes. The composition of lipid bilayers and their "fluidity" directly govern both the passive transport of drugs, metabolites and other nonelectrolyte solutes (1–2) and the activity and kinetics of membrane-bound enzymes and carriers (3–4). Isolated planar black lipid membranes (BLM) formed from a solution of a lipid dispersed in a nonpolar solvent such as *n*-decane (5) have become important model systems for the study of various biomembrane phenomena. In contrast to biological membranes, the chemical composition and structure of isolated lipid bilayers are generally more readily established, which offers advantages in studies of transport mechanisms.

Unlike the isotropic environment encountered by a solute diffusing in a bulk solvent or through a homogeneous membrane, the microenvironment encountered by a molecule permeating through a lipid bilayer membrane varies dramatically with depth. In its transit through a bilayer, a permeant encounters three somewhat distinct domains: an ordered, highly polar interfacial (head group) region, an outer, well-ordered hydrocarbon region, and a region of relatively disordered hydrocarbon chains near the center of the bilayer. The disordered hydrocarbon interior may be expanded in thickness by as much as twofold in planar lipid bilayer membranes formed from a phospholipid dissolved in hydrocarbon due to the accumulation of excess hydrocarbon solvent in the bilayer interior.

An as yet unresolved issue, central to a complete understanding of molecular permeability through lipid bilayer membranes, is the degree to which each of these domains contribute to the overall barrier properties. Two experimental techniques which address this question are developed and used in this paper to explore the barrier properties of lecithin/decane bilayers. First, the thickness of lecithin/decane bilayers has been systematically varied by modulating the chemical potential of decane in the annulus surrounding the bilayer using different mole fractions of squalene in decane. Using these bilayers, the dependence of permeability of a model permeant (acetamide) on the thickness of the disordered hydrocarbon region of the bilayer has been assessed to determine the contribution of this region to bilayer resistance.

The relative contributions of the bilayer interface and ordered hydrocarbon regions to the transport barrier may be evaluated by exploring the effective chemical nature of the rate determining barrier microenvironment. This may be probed by comparing functional group contributions to solute transport through bilayers with those obtained for partitioning of the same solutes between water and various model bulk solvents ranging from nonpolar hydrocarbons to polar, hydrogen-bonding solvents such as octanol. Because permeabilities for a series of compounds in which even a single substituent is varied may span several orders of magnitude, group contributions for a wide range of substituents are difficult to

obtain. At low permeabilities limitations arise from difficulties in detection of transported permeant; at high permeabilities, unstirred water layers become rate limiting in transport experiments. Described herein is a novel approach for obtaining group contributions to transport using ionizable permeants and pH adjustment to identify for each permeant a pH "window" in which transport is clearly membrane controlled and fluxes are sufficiently high to allow accurate detection of permeant concentration in the receiver compartment of a transport cell. Using this procedure, the -OH group contribution to transport through a lecithin/bilayer has been determined.

## METHODS AND MATERIALS

### Bilayer thickness determinations

Lipid bilayer thickness was determined by capacitance measurements using an electrochemical system developed in this laboratory. A circuit diagram is shown in Fig. 1. A four-electrode system (two silver-silver chloride reference electrodes and two platinum working electrodes) was placed in the diffusion cell to maintain a stable potential on both sides of the membrane by the feedback circuit in a potentiostat (Model JDP 165A, JAS). A sine wave signal from an 11 MHz stabilized function generator (Model 21, Wavetek, Barnhill Corporation, Inc., Murray, UT) is split into two parts, one passing through a lock-in amplifier (Ithaco Model 3941, Ithaco, Inc., Ithaca, NY) as a reference signal and the other passing through the potentiostat and then the membrane. Any unwanted impedance contribution from the electronic system alone is eliminated by adjusting the corresponding amplitude ( $A$ ) and phase ( $\phi$ ) to zero. The amplitudes and phase shifts for a standard capacitor ( $A_0$ ,  $\phi_0$ ) and the membrane system ( $A_m$ ,  $\phi_m$ ) can be measured for frequencies ranging from 10 Hz to 500 kHz. Compared with the traditional AC bridge (6-7) and the DC transient relaxation methods (8), the present technique has the advantage of greatly enhanced data acquisition and noise reduction.

The working equations relating the complex capacitance  $C_m^*$ ,

$$C_m^* = C' - jC'', \quad (1)$$

of the membrane system to the experimentally observable data ( $A_m$ ,  $\phi_m$ ) are (cf Appendix)

$$C' = C_0 \frac{A_m}{A_0} \cos(\phi_m - \phi_0), \quad (2)$$

and

$$C'' = C_0 \frac{A_m}{A_0} \sin(\phi_m - \phi_0), \quad (3)$$

where  $C_0$  is the capacitance of the standard capacitor. Cole-Cole plots are obtained by plotting  $-C''$  versus  $C'$  at different frequencies,  $f$ . The limiting value of  $C'$  as  $f \rightarrow 0$  gives membrane capacitance  $C_m$  plus a small contribution from stray capacitance of the electronic system.

The planar lipid bilayer can be treated as a parallel plate capacitor with the capacitance

$$C_m = \frac{\epsilon_0 \epsilon_m S_m}{d_m}, \quad (4)$$

where  $\epsilon_0 = 8.854 \times 10^{-12}$  F/m,  $\epsilon_m$  is the effective membrane dielectric constant,  $d_m$  is the effective membrane thickness, and  $S_m$  is the bilayer area. The head groups in the bilayer, which have high dielectric

constant and can be considered to be in series with the hydrocarbon interior, have only a minor contribution to the measured capacitance (6-7).

### Bilayer area measurements

The absolute area of the Teflon hole used for the bilayer formation was determined by using vernier microcalipers. To measure the area of the "black" (bilayer) portion of lipid films during the transport experiments, membranes were viewed through a StereoZoom microscope (Bausch and Lomb, Rochester, NY) aligned normal to the membrane. Photographs were made on Polaroid 667 (ASA 300) film with a 3-1/4 × 4-1/4" Polaroid Land camera (Bausch and Lomb, Rochester, NY). The membrane was transilluminated with an illuminator (Model 650, Reichert Scientific Instruments, Buffalo, NY). After photographing the membrane, the area of the bilayer was determined by the weight-area method.

### Permeability coefficient determinations

Lipid membranes were made by applying a lipid solution across a 1-2 mm diameter hole in a Teflon sheet separating two water-jacketed chambers. The temperature in both chambers was maintained at  $25.0 \pm 0.05^\circ\text{C}$  by a combined refrigerated water bath/circulator (Haake A81, Haake Inc., NJ) and flow system (Masterflex, Cole-Parmer Instruments Co., Chicago, IL). Both chambers contained ~4.0 ml buffered aqueous solution and were stirred continuously with magnetic fleas during the course of the experiment. The buffer solutions used were 0.01 M HEPES, MES or formic acid depending on the pH range used. The ionic strength was held at  $I = 0.1$  with NaCl. The pH in the donor chamber was monitored with a micro-combination pH probe (MI-412, Microelectrodes, Inc., Londonderry, NH) and was found to be stable ( $\pm 0.01$ ) during each experimental run.

To detect trace amounts of solutes transported through the bilayer membranes, a radiotracer method was first used. After the lipid bilayer was formed and a constant capacitance across the membrane was attained, a small amount ( $\sim 10 \mu\text{l}$ ) of a radioisotope-labeled compound was injected into the donor chamber. Samples taken from both chambers at certain intervals were mixed with Aquasol scintillation cocktail (Opti-Fluor, Packard Instrument Co., Inc., Meriden, CT) and counted in a liquid scintillation counter (Beckman LS 1801, Beckman Institute, Fullerton, CA).

As impurities in radiolabelled permeants, even in small amounts, can significantly increase observed permeabilities and their contribution cannot be corrected for properly, a new method using high performance liquid chromatography (HPLC) was developed to detect transported permeant. After thinning of membranes was completed, a small amount ( $\sim 50 \mu\text{l}$ ) of solution with "cold" permeant at a known concentration was added to the donor chamber and a corresponding volume of buffer was added to the receiver chamber. The substrate concentration in the donor chamber was about  $1 \times 10^{-3}$  M. Samples were withdrawn from both chambers at various intervals and adjusted to pH  $\sim 3$  by addition of a small amount 0.1 N HCl. The samples from the donor chamber were appropriately diluted to bring the solute concentrations within a linear absorbance range and samples taken from both chambers were then analyzed by HPLC as described in a later section.

Permeability coefficients were calculated from the slopes of plots of receiver concentration  $C_{\text{receiver}}$  versus time interval  $\Delta t$  according to the following equation

$$P_e = \text{slope} \times \frac{V_{\text{cell}}}{S_m C_{\text{donor}}}, \quad (5)$$

where  $P_e$  is the apparent permeability coefficient,  $V_{\text{cell}}$  is the volume of the aqueous solution in each chamber and  $C_{\text{donor}}$  is the concentration of the solute in the donor chamber. Point-by-point areas  $S_m$  were monitored continuously during the experiments either microscopically or by

### CIRCUIT DIAGRAM

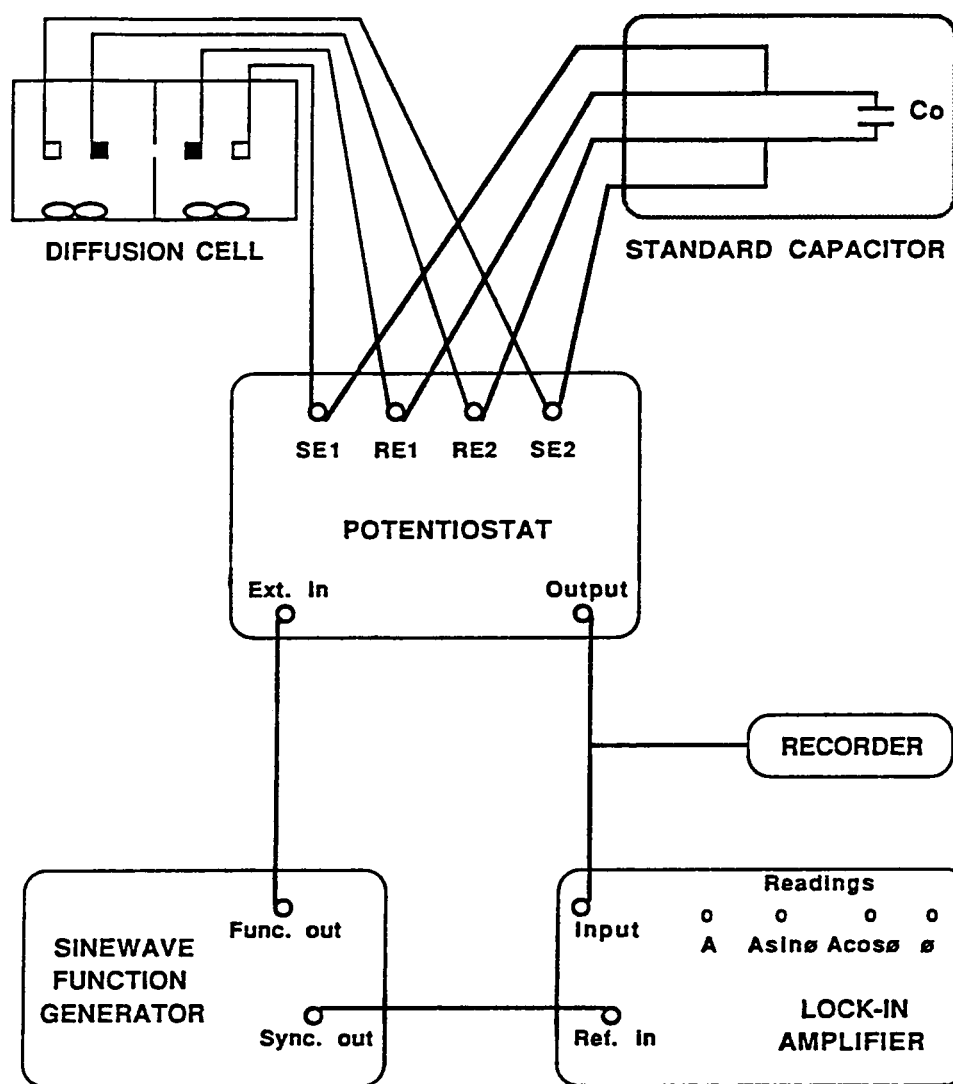


FIGURE 1 An electrochemical system developed in this laboratory for membrane capacitance measurements.

the capacitance method described above. Permeability coefficients were calculated using the average  $S_m$  over each time interval.

### Partition coefficient determinations

The partition coefficient for acetamide between water and decane was determined in duplicate using  $^3\text{H}$ -acetamide. Approximately  $10\ \mu\text{Ci}$  of acetamide was dissolved in 1 ml deionized water in a 5 ml centrifuge tube and 3 ml decane was then added. After vigorous mixing and centrifugation, the sample was allowed to stand in a thermal bath ( $25 \pm 0.05^\circ\text{C}$ ) for 48 h. After aliquots were taken from both phases and counted in a scintillation counter, the original decane layer was replaced with fresh decane and the above procedure was repeated to ensure that hydrophobic contaminants had not caused a large error in the initial partition coefficient determination. No significant quantity of hydrophobic contaminants was found by this procedure.

The partition coefficients for *p*-toluic acid and *p*-hydroxymethyl benzoic acid between water and either hexadecane or octanol were measured at  $25^\circ\text{C}$  using "cold" compounds. The samples taken from both phases were appropriately diluted and analyzed by HPLC. The

pH in the aqueous phase was maintained well below the solutes'  $\text{pK}_a$  values by 0.01 M HCl so that more than 99% of the substrates were in their unionized form.

### Diffusion coefficient measurements

To estimate the effects of unstirred aqueous layers and the hydrocarbon solvent entrapped between the two monolayers on the overall transport rate through the bilayer membrane, diffusion coefficients of solutes in the relevant solution systems are required. The diffusion coefficients for acetamide and *p*-toluic acid were determined in this study by an open-ended capillary method introduced by Anderson et al. (9). In contrast with the diaphragm-cell and porous porcelain frit methods, the present method has the advantages of being an absolute method and having a small surface to volume ratio so that solute adsorption effects are small. The diffusion capillaries used were  $\sim 0.6$  mm in internal diameter and 5 cm in length (1). Before diffusion four capillaries were filled with the same solution of known solute concentration ( $< 1 \times 10^{-3}$  M). They were then immersed vertically into a reservoir ( $\sim 1$  liter) containing the same solution but without solute. The

reservoir was placed in a large circulating bath controlled at a temperature of  $25 \pm 0.05^\circ\text{C}$ . After diffusion had taken place for a certain length of time ( $t$ ), the capillaries were withdrawn from the reservoir and the solution in each capillary was removed with a  $10\text{-}\mu\text{l}$  microsyringe and dissolved in 1 ml water. The capillaries were rinsed several times. The concentration ( $C_i$ ) was then determined either by counting radioactivity or by HPLC. The diffusion time was selected such that  $D_s t/l^2 > 0.2$ . Under this condition, a simple relationship exists between  $D_s$  and  $C_i$ ,

$$D_s = \frac{4l^2}{\pi^2 t} \ln \left[ \left( \frac{8}{\pi^2} \right) \left( \frac{C_0}{C_i} \right) \right], \quad (6)$$

where  $C_0$  is the initial concentration of the solute in the capillaries.

## HPLC analyses

An HPLC system consisting of a syringe-loaded sample injector (Rheodyne Model 7125, Rainin Instrument Co., Woburn, MA) with  $100\text{-}\mu\text{l}$  loop, a solvent pump (Model 110A; Beckman Instruments, Inc., Fullerton, CA), a dual-wavelength absorbance detector (Model 441; Waters Associates, Milford, MA) operated at 254 nm, an integrator (Model 3392A, Hewlett-Packard Co., Avondale, PA), and a reversed-phase column packed with  $5\text{ }\mu\text{m}$  Spheri-5 RP-18 (Brownlee OD-MP,  $4.6\text{ mm ID} \times 10\text{ cm L}$ ; Rainin) was used at ambient temperature for the analyses of the samples taken from the transport, partition and diffusion experiments. The mobile phase contained acetonitrile in deionized water and was buffered to a pH of  $\sim 3.0$  using  $0.02\text{ M}$  phosphate buffer. The ratio of organic to aqueous phase was 15% for *p*-hydroxymethyl benzoic acid and 30% for *p*-toluic acid.

## Materials

Egg lecithin in chloroform ( $20\text{ mg/ml}$ ) obtained from Avanti Polar-Lipids, Inc. (Pelham, AL) was dried under nitrogen gas and dispersed (2% w/v) in solvent. The solvents decane (99+%, Sigma Chemical Co., St. Louis, MO) and squalene (98 ~ 100%, Sigma) were passed through an alumina column before use.  $^{14}\text{C}$ -*p*-toluic acid (New England Nuclear, Boston, MA) was used as purchased.  $^3\text{H}$ -*p*-hydroxymethyl benzoic acid was obtained as a crude product from Amersham International plc, Amersham, UK and was purified by HPLC. The purified samples were stored in solution at pH = 8 to prevent the samples from degradation.  $^3\text{H}$ -acetamide was synthesized in our laboratory by a reaction of  $10\text{ mmol}$   $^3\text{H}$ -acetic anhydride (New England Nuclear, Boston, MA) with  $60\text{ mmol}$   $\text{NH}_4\text{OH}$  (30% in  $\text{H}_2\text{O}$ ) and the crude product was purified by HPLC.

## RESULTS AND DISCUSSION

### Variation of bilayer thickness by modifying the activity of decane in the annulus

It is well known that residual hydrocarbon solvent used in the formation of thin lipid membranes remains in the bilayer after the thinning process resulting in an increased thickness (10–11). Questions remain, however, as to how this solvent, which is not present in biomembranes, affects transport through bilayers. Fig. 2 depicts the essential elements in a typical lipid membrane. Differential scanning calorimetry (10), x-ray diffraction (10), and  $^2\text{H}$ -NMR (11) measurements indicate that the solvent trapped in the bilayer is located mainly in the less ordered central region. Alkanes differing in chain length are not equally soluble in lipid bilayer membranes (12) and the local order parameters do not vanish (13) sug-

gesting that the solvent filled bilayer interior may be similar but is not completely equivalent to a simple bulk liquid hydrocarbon.

The thickness of most lipid bilayers formed with egg lecithin in decane spans the range of  $41 \sim 51\text{ }\text{\AA}$ . To extend the thickness range one can use as a dispersion medium either one-component hydrocarbon solvents differing in chain length (12) or solvent mixtures differing in mole fraction of the composite components (14). Solvent mixtures made of different mole fractions of squalene in decane were used in this study. The method was first introduced by White (14) to obtain "solvent-free" bilayers made of glyceryl monooleate. The bilayer itself is assumed to be free of squalene as a previous study has shown that squalene is insoluble in dipalmitoyl lecithin dispersions (15). The presence of squalene in the annulus can, however, modify the chemical potential of decane in the annulus which is in metastable thermal equilibrium (16) with the bilayer and thus determine the solubility of decane in the bilayer because of the enormous mass difference between the bilayer and its surrounding torus. The thickness of the bilayer  $d_m$  is directly correlated with the solubility of decane in the bilayer,

$$d_m = n_L V_L + n_D V_D, \quad (7)$$

where  $n_L$  and  $n_D$  are the number of lipid and decane molecules per unit area of bilayer, respectively, and  $V_L$  and  $V_D$  are the molecular volumes of the lipid and decane. Fig. 3 shows capacitance-area profiles for bilayer membranes with different mole fractions of squalene in decane. As expected, the observed capacitances correlate linearly with the bilayer areas with slopes giving specific capacitances of the bilayer membranes. Fig. 4 shows the variation of the bilayer thickness at different mole fractions of squalene ( $X_{sq}$ ) in decane, determined from specific capacitances. The bilayer membranes formed have thicknesses ranging from  $25\text{ }\text{\AA}$  to  $51\text{ }\text{\AA}$ . For  $X_{sq} < 0.3$  the bilayer membranes formed were stable for up to several hours, whereas for  $X_{sq} > 0.4$  the membranes were difficult to form and once formed did not have a stable area but expanded continuously at the expense of the surrounding torus. The lower limit of the bilayer thickness obtained with  $X_{sq} = 0.3 \sim 0.4$  ( $d_m = 25\text{ }\text{\AA}$ ) is very similar to that deduced from x-ray diffraction measurements on the lamellar phase of lecithin ( $d_m = \sim 26\text{ }\text{\AA}$ , [17–19]), implying that essentially solvent-free bilayer membranes are formed under these conditions.

### Permeability of acetamide: assessment of the effects of bilayer thickness, unstirred water layers, and the annular region on $P_m$

It is well established from NMR studies (13, 20) that the structural ordering ( $S_{CD}$ ) and motional relaxation ( $T_1$ ) of local segments in lipid bilayer membranes have plateau values for most of the alkyl chain and then decrease rap-

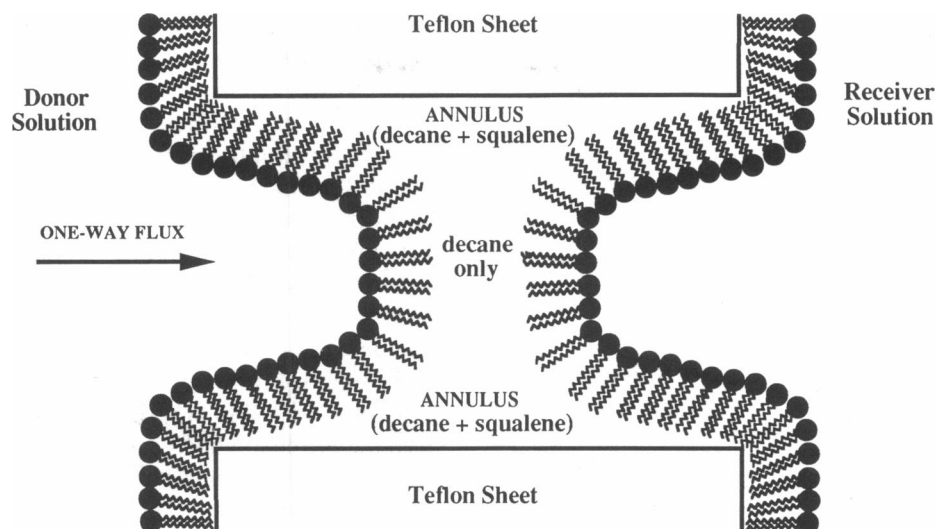


FIGURE 2 A schematic depiction of a typical lipid membrane system.

idly near the tail of the chain. This result provides a basis for separating the bilayer interior into two regions, one being a highly ordered region with an average solute diffusion coefficient and partition coefficient of  $D_{\text{order}}$  and  $K_{\text{order}}$ , and the other being a disordered region, including also the trapped solvent, with an average solute diffusion coefficient and partition coefficient of  $D_{\text{disorder}}$  and  $K_{\text{disorder}}$ .

Following a kinetic integral equation for nonelectrolyte permeation proposed by Diamond and Katz (21), the permeability ( $P_m$ ) through a symmetric membrane can be written as

$$\frac{1}{P_m} = \frac{2}{k_i} + \frac{d_{\text{order}}}{K_{\text{order}} D_{\text{order}}} + \frac{d_{\text{disorder}}}{K_{\text{disorder}} D_{\text{disorder}}}, \quad (8)$$

where  $k_i$  is the rate constant for interfacial transport and  $d_{\text{order}}$  and  $d_{\text{disorder}}$  are the effective thicknesses of the or-

dered and disordered regions, respectively. If the disordered region, which may account for up to 50% of the thickness in lecithin/decane bilayers due to the entrapped solvent, represents a significant barrier to diffusion, an inverse dependence of permeability on bilayer thickness should be evident.

The thickness dependence of the permeabilities ( $P_m$ ) for acetamide through lecithin/decane + squalene bilayers is shown in Fig. 5. Thicknesses were varied by using different mole fractions of squalene in decane as described previously. In the figure, the solid line is a plot consistent with Overton's rule

$$P_m = K_{w \rightarrow m} D_m / d_m, \quad (9)$$

where  $K_{w \rightarrow m}$  is the permeant lipid bilayer/water partition coefficient. For this comparison the predicted curve was forced through the average observed permeability coefficient at a bilayer thickness of  $d = 50$  Å. While Overton's rule assumes the bilayer to be a homogeneous phase and

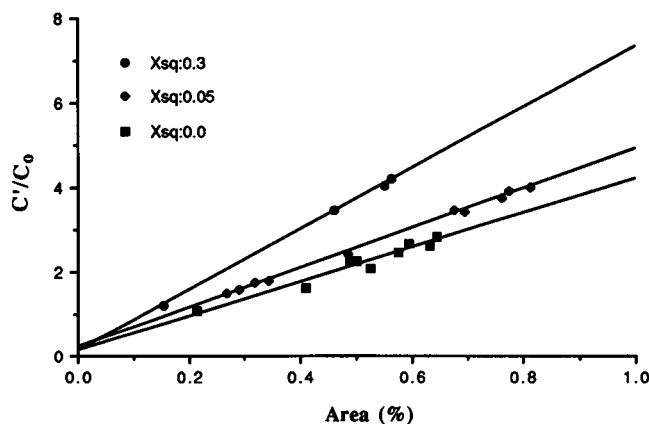


FIGURE 3 The real part of  $C'$  of the complex capacitance  $C_m^*$  at  $f \rightarrow 0$  versus bilayer area in percentage. Shown are the three lipid membranes formed with different mole fraction of squalene in decane,  $X_{sq} = 0.0$ ,  $0.05$ , and  $0.3$ .

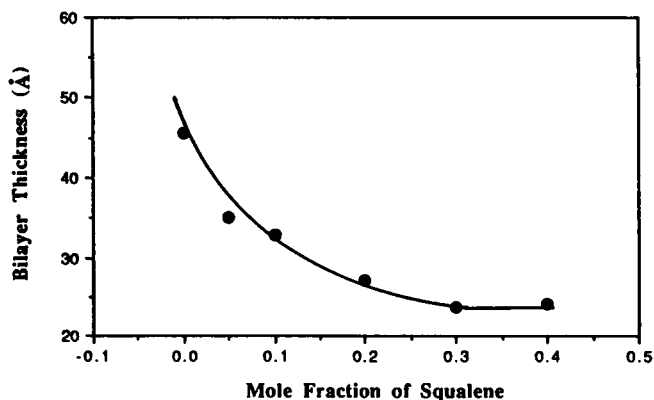


FIGURE 4 The variation of the bilayer thickness with different mole fractions of squalene in decane.

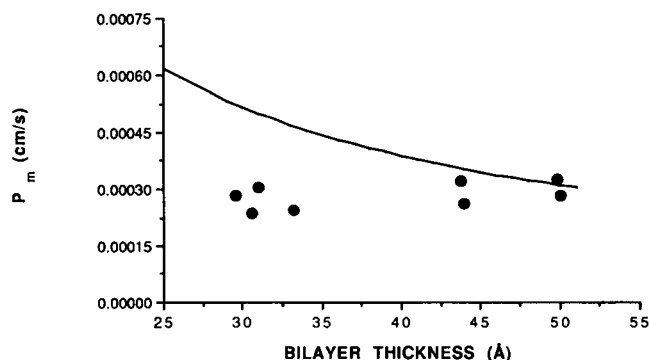


FIGURE 5 The permeability coefficient of acetamide at 25°C as a function of bilayer thickness. The bilayer thickness was varied by using different mole fractions of squalene in decane as a dispersion medium for the lipid.

thus predicts that the transport rates through lipid bilayers are inversely proportional to the bilayer thickness, our experimental results exhibit no significant dependence on the bilayer thickness.

Several possibilities may account for this observation: (a) the flux of acetamide may be unstirred water layer controlled under the conditions of this experiment; (b) the flux of acetamide through the annular region surrounding the bilayer may predominate and mask the effects of thickness in the bilayer region; (c) the transport of acetamide through the hydrocarbon region in the center of the bilayer is rapid relative to transport through other domains; or (d) the organization of chains in the peripheral region of the bilayer or at the bilayer/water interface is perturbed by decane in a manner which exactly cancels the decrease in permeability coefficient resulting from an increase in thickness. Each of these possibilities are now considered in more detail.

The total unstirred water layer thickness in our transport cell was determined (see later discussion) to be  $170 \pm 8 \mu\text{m}$ , yielding a thickness ratio for unstirred water layers to a lecithin/decane bilayer having maximum thickness ( $d_m \sim 50 \text{ Å}$ ) of  $\sim 34,000$ . Small, relatively lipophilic molecules are therefore likely to exhibit unstirred water layer controlled transport across planar bilayer membranes. Acetamide was chosen as a model permeant for these studies because it is relatively hydrophilic and therefore, likely to be membrane controlled in its transport. The diffusion coefficient of acetamide in water was found by the open-ended capillary method to be  $(1.41 \pm 0.02) \times 10^{-5} \text{ cm}^2 \text{ s}^{-1}$  at  $25 \pm 0.05^\circ\text{C}$ , which is in good agreement with the data reported by Gary-Bobo and co-workers of  $(1.32 \pm 0.03) \times 10^{-5} \text{ cm}^2 \text{ s}^{-1}$  at  $24.8 \pm 0.05^\circ\text{C}$  (22). From the diffusion coefficient and unstirred water layer thickness an apparent permeability coefficient of  $8.3 \times 10^{-4} \text{ cm s}^{-1}$  would have been expected for acetamide if its transport were unstirred water layer controlled. The observed average permeability coefficient of  $(2.2 \pm 0.2) \times 10^{-4} \text{ cm s}^{-1}$  de-

termined for acetamide in lecithin/decane bilayers at maximum thickness is approximately 25% of the unstirred water layer estimate. We conclude, therefore, that the flux of acetamide is primarily lipid bilayer membrane controlled in these experiments. Correcting for the unstirred layer contribution, we obtain a membrane permeability coefficient,  $P_m = (2.9 \pm 0.3) \times 10^{-4} \text{ cm s}^{-1}$ . This value is comparable to the value ( $P_m = 1.7 \times 10^{-4} \text{ cm s}^{-1}$ ) reported by Orbach and Finkelstein (2) under similar experimental conditions. The discrepancy may be attributed to many factors, one being the poorer temperature control ( $\pm 2^\circ\text{C}$ ) in the work cited.

Referring to Fig. 2, it is evident that a permeant may pass from the donor to receiver compartment through the thin bilayer region or through the thick torus surrounding the bilayer. In any given experiment the area which thins to bilayer dimensions may be a small fraction of the area occupied by this annulus. The interior of the latter consists mainly of solvent and is therefore hydrocarbonlike in its properties. If diffusion through this region is fast relative to the rate of permeant transfer across the interfacial or more ordered hydrocarbon regions adjoining the interface, it is conceivable that the flux of acetamide reflects primarily *trans*-annular diffusion. This could account for the absence of any dependence of acetamide flux on bilayer thickness. However, White has shown by a thermodynamic argument that the torus is sufficiently thick that it has a negligible effect on the capacitance measurement of bilayer thickness (23), supporting the view of Stein (24) that the torus is many times thicker than the black membrane and would not normally present a significant parallel pathway for diffusion. We have shown that the flux of acetamide depends linearly on the area of the black portion of the membrane and approaches zero as the area of the bilayer region approaches zero. Fig. 6 presents the observed permeability coefficient of acetamide per unit area of the bilayer portion of lecithin/decane bilayers as a

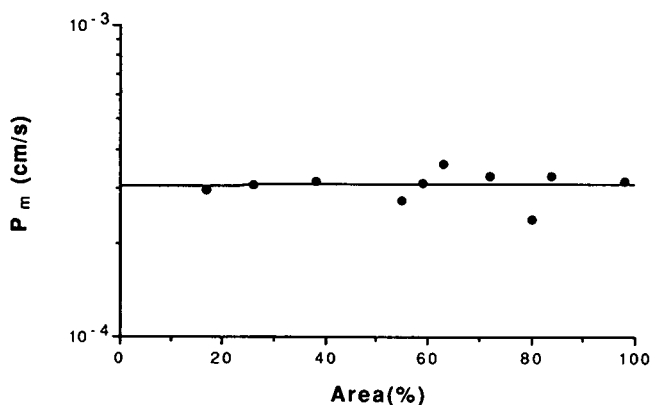


FIGURE 6 The permeability coefficient (= flux divided by bilayer area) of acetamide at 25°C as a function of bilayer area. The bilayer membranes were made of egg lecithin (2% w/v) in decane.

function of bilayer area expressed as a percentage of total film area. There is no detectable change in permeability coefficient per unit area over a range of bilayer area percentages from ~15% to nearly 100%. The transport rates therefore reflect trans-bilayer diffusion.

Given that the permeability coefficients reported for acetamide reflect its transport across the bilayer region, it appears likely from the lack of dependence in these values with bilayer thickness that the hydrocarbon solvent interior does not contribute substantially to the barrier. We may estimate the permeability through the core hydrocarbon region ( $P_0$ ) by the following expression

$$P_0 = \frac{K_{w \rightarrow 0} D_0}{d_0} \quad (10)$$

$K_{w \rightarrow 0}$  is the decane/water partition coefficient using molar concentrations, which we have determined to be  $0.93 \times 10^{-5}$ . The diffusion coefficient  $D_0$  for acetamide in decane was estimated by plotting diffusivities of *n*-alkanes ( $C_1 \sim C_7$ ) at 25°C in decane (25) versus molar volume and interpolating the diffusivity at the estimated molar volume for acetamide. This procedure gives  $D_0 = 3.2 \times 10^{-5} \text{ cm}^2 \text{ s}^{-1}$ . With a maximum hydrocarbon core length of  $d_0 \sim 25 \text{ Å}$ , we have  $P_0 = 1.2 \times 10^{-3} \text{ cm s}^{-1}$ . The ratio  $P_m/P_0$  is then equal to 0.24 at the maximum core thickness. These calculations are consistent with the absence of a significant effect of bilayer thickness on acetamide's permeability coefficient.

Whereas the torus surrounding the bilayer is several orders of magnitude thicker than the bilayer,  $P_m$  is only 4–5 times smaller than  $P_0$ . This fact provides further evidence that the torus surrounding the bilayer membrane should have a negligible effect on the overall transport rate of acetamide, and is consistent with the linear dependence of permeability coefficient on the area of the bilayer portion of the membranes examined.

It is possible that the lack of dependence of acetamide's permeability on bilayer thickness reflects a fortuitous cancellation of the effect of thickness predicted by Overton's rule and an enhancement caused by perturbation of the ordered regions of the bilayer with increasing solvent content. Variation in hydrocarbon content in the bilayer membrane is expected to have only a minor effect on the lipid chain organization in the bilayer since the solvent is mainly located between the two lipid monolayers. This is in agreement with surface density measurements (12) which found that the area per molecule ( $61 \text{ Å}^2$ ) of lecithin does not vary significantly with chain lengths of the hydrocarbon solvent used, even though bilayer thickness varies substantially. However, recent studies by De Young and Dill (26–27) indicate that solute (benzene and hexane) partitioning between a phospholipid bilayer and water decreases by an order of magnitude as the surface density increases by only two fold. Thus, it appears that a very slight decrease in surface density with increasing solvent content in the bilayer,

which may have been obscured in previous studies due to inherent experimental uncertainties and/or theoretical assumptions, could significantly affect the observed permeability. The range over which acetamide's permeability coefficient remains independent of thickness would appear to make this possibility unlikely, however.

A study by Marqusee and Dill (28) has shown that local anisotropy in bilayer membranes has important consequences relating to the distribution of substrates within the bilayer interior. Independent of molecular polarity, a substrate molecule tends to localize preferentially in the mid-layer region rather than in the more ordered regions. If the discrepancy between the permeabilities  $P_m$  and  $P_0$  is solely due to unfavorable partitioning into the ordered regions, one has the following relation (28)

$$P_m = qP_0, \quad (11)$$

where  $q$  is a multiplying factor reflecting the unfavorable statistical weight for a chain segment in the ordered domain. For a surface density of  $61 \text{ Å}^2/\text{molecule}$  and an average chain length of 17.8 carbons in the egg yolk phosphatidyl choline (12), an average weight  $q$  of 0.18 is obtained from interpolation of the results of Marqusee et al. (28). One thus has  $P_m/P_0 = 0.18$ . This theoretical prediction is in reasonable agreement with our experimental result and suggests that the ordered hydrocarbon region (2nd term in Eq. 8) is an important component of bilayer membrane resistance.

## Determination of functional group contributions to transport

The effects of various substituents on permeant transport through lipid bilayers when compared with the effects of the same substituents on organic solvent/water partition coefficients as the organic phase is varied from relatively nonpolar to polar, hydrogen-bonding solvents may provide useful information on the chemical microenvironment probed by the permeant in the rate-limiting region of the bilayer. Particularly, we wish to know whether the rate-limiting microenvironment is hydrocarbonlike, as one might expect if the ordered hydrocarbon region is the barrier to transport, or a more polar, hydrogen-bonding region such as that likely to be found in the interfacial region of a bilayer. Reliable functional group contribution data for bilayer membrane transport are now available only for the  $-\text{CH}_2-$  group over a narrow range of solute chain lengths and in a limited number of bilayer systems (29).

The contribution of a functional group,  $X$ , to the standard free energy of solute transfer from water to an organic solvent may be expressed by

$$\Delta(\Delta G^0)_X = -RT \ln (K_{w \rightarrow 0}^{\text{RX}}/K_{w \rightarrow 0}^{\text{RH}}), \quad (12)$$

where  $K_{w \rightarrow 0}^{\text{RX}}$  and  $K_{w \rightarrow 0}^{\text{RH}}$  are the solvent/water partition coefficients for the substituted and unsubstituted solute

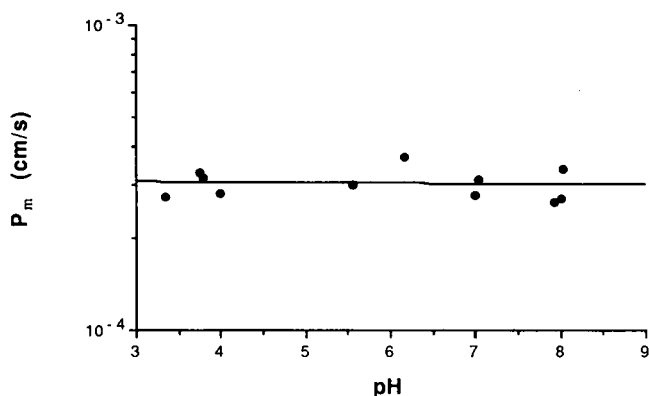


FIGURE 7 The permeability coefficient of acetamide at 25°C as a function of solution pH. The pH was controlled by 0.01 M HEPES, MES or formic acid, depending on the pH range used. The ionic strength was held at  $I = 0.1$  with NaCl.

molecules, respectively. Similarly, an apparent functional group contribution to the standard free energy of permeant transfer from water to the rate-limiting domain of a lipid bilayer may be obtained from the membrane permeability coefficients of a substituted and unsubstituted permeant,  $P_m^{RX}$  and  $P_m^{RH}$ , respectively

$$\Delta(\Delta G^0)_X = -RT \ln (P_m^{RX}/P_m^{RH}). \quad (13)$$

If both polar, hydrogen-bonding substituents as well as nonpolar substituents are included within a series of permeants, permeability coefficients are likely to vary by several orders of magnitude. More lipophilic members of the series are therefore likely to be unstirred water layer controlled while transport of the most polar compounds may be difficult to detect. This problem has been circumvented in this study by utilizing *p*-toluic acid as the unsubstituted reference permeant. A comparison of the membrane controlled permeability of this compound with that of *p*-hydroxymethyl benzoic acid has allowed us to calculate the  $-\text{OH}$  group contribution to transport.

*p*-toluic acid in its unionized form exhibits aqueous diffusion controlled transport across lipid bilayer membranes. However, as the fraction of unionized species is decreased with increasing solution pH, the transport of *p*-toluic acid becomes membrane controlled (permeability decreases), establishing that it is the neutral species which accounts for bilayer flux.

To ensure that variation in pH does not alter the barrier properties of lecithin/decane bilayers, the permeability coefficient for acetamide, a nonelectrolyte, was determined over the pH range 3–8. Fig. 7 shows that the permeability of acetamide is constant over this range, indicating that pH does not affect the resistance of lecithin/decane bilayers.

Permeability-pH profiles for *p*-toluic acid and *p*-hydroxymethyl benzoic acid are presented in Fig. 8. Both radiotracer and HPLC methods were used to obtain

fluxes for *p*-hydroxymethyl benzoic acid across the bilayer membranes and were found to agree closely with each other. Under conditions of low permeability ( $P < 10^{-4}$  cm/s) the two methods diverged with increasing pH, with apparent permeability coefficients obtained by the non-specific radiotracer method exceeding those obtained by HPLC. This divergence was attributed to contributions of impurities to the apparent flux of radiotracer. The HPLC method developed in this study has the following merits: (a) Since only “cold” compounds are required, the selection of compounds for study is less constrained by availability; (b) the effects of impurities on transport rates are eliminated; and (c) the permeation rates of more than one permeant can be determined in a single transport experiment as long as the permeants do not affect membrane barrier properties and do not interact with each other either in solution or in the membrane. This can be verified by measuring permeation rates at various permeant concentrations.

At steady state, assuming equilibrium between species in the unstirred aqueous layers and that only the unionized species cross the membrane, the observed permeabilities ( $P_e$ ) are related to the true permeability coefficient ( $P_m^{HA}$ ) through the bilayer membrane by (30–31)

$$\frac{1}{P_e} = \frac{1}{P_m^{HA} f_{HA}} + \frac{d_{ul}}{D_{aq}}, \quad (14)$$

where  $f_{HA}$  is the fraction of the unionized species HA and  $d_{ul}$  and  $D_{HA}$  are, respectively, the entire unstirred water layer thickness and the aqueous diffusion coefficient for HA. The difference in the aqueous diffusion coefficients of the neutral and ionic forms,  $D_{HA}$  and  $D_A$ , is generally on the order of a few percent (32) and thus we assume that  $D_{HA} = D_A$ .  $f_{HA}$  is determined at a given pH from the ionization constant of HA,  $K_a$ . The  $\text{p}K_a$  for *p*-toluic acid at infinite dilution at 25°C is 4.36 (33). A correction for the ionic strength of 0.1 gives  $\text{p}K_a = 4.25$ . The  $\text{p}K_a$  for

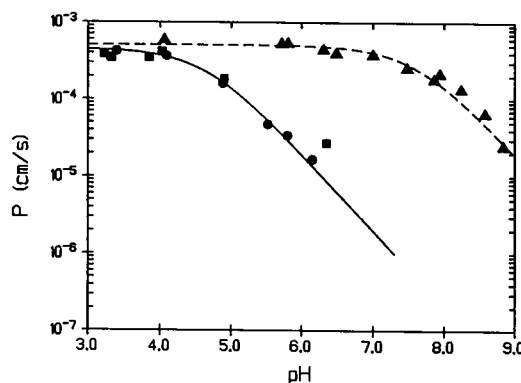


FIGURE 8 The permeability-pH profiles for both *p*-toluic acid ( $\blacktriangle$ ) and *p*-hydroxymethyl benzoic acid ( $\bullet$ ,  $\blacksquare$ ) at 25°C. Both radiotracer ( $\blacksquare$ ) and HPLC ( $\bullet$ ) methods were used to determine the permeability coefficient of *p*-hydroxymethyl benzoic acid. Both solid and dashed lines are from nonlinear regression analyses using Eq. 14.



TABLE 1 Permeability coefficients  $P_m$ , partition coefficients  $K_{w \rightarrow o}$ , and ionization constants  $K_a$  at 25°C for solutes examined in this study\*

Substrate	$P_m$ (cm/s)	$K_{w \rightarrow o}$			$K_a$
		Saturated hydrocarbon/water	Hexadecene/water	Octanol/water	
Acetamide	$(2.9 \pm 0.3) \times 10^{-4}$	$9.3 \times 10^{-6}\ddagger$	—	—	—
<i>p</i> -toluic acid	$1.1 \pm 0.2$	$(2.61 \pm 0.02) \times 10^{-1}\S$	$(5.18 \pm 0.06) \times 10^{-1}$	$230 \pm 3$	$4.37 \times 10^{-5}$
<i>p</i> -hydroxymethyl benzoic acid	$(1.6 \pm 0.4) \times 10^{-3}$	$(5.31 \pm 0.20) \times 10^{-5}\S$	$(2.45 \pm 0.05) \times 10^{-4}$	$8.51 \pm 0.14$	$6.31 \times 10^{-5}$

\* Expressed as mean  $\pm$  standard deviation;  $\ddagger$  decane/water partition coefficient;  $\S$  hexadecane/water partition coefficient.

*p*-hydroxymethyl benzoic acid was measured in our laboratory by an acid-base titration, yielding  $pK_a = 4.20$ . Similarly, at 0.1 ionic strength  $pK_a = 4.09$ . Equation 14 is valid only if the  $H^+$  concentrations across the unstirred layers remain constant. Deviation from this ideal circumstance may occur when the transport flux is high and the buffer capacity is low. We have developed a diffusion kinetic model to calculate the concentration profiles of the relevant species in the unstirred layers. Given all the experimental conditions, our model calculations indicate that the relative error in the observed permeability due to differences in pH within the unstirred water layers is negligible compared with the experimental uncertainty. This is further verified by our initial control experiments in which the permeability coefficient for *p*-hydroxymethyl benzoic acid was measured at several donor concentrations spanning the range of  $(0.5 \sim 6) \times 10^{-3}$  M. No significant variation in permeability coefficients was observed.

Because of the better statistical precision in *p*-toluic acid's permeability data, its regression analysis was used to estimate the thickness of the entire unstirred layer,  $d_{ui} = (170 \pm 8) \mu\text{m}$ . The diffusion coefficient for *p*-toluic acid in water was determined by the open-ended capillary method to be  $(8.7 \pm 0.2) \times 10^{-6} \text{ cm}^2 \text{ s}^{-1}$ . Nonlinear fits of the pH profiles in Fig. 8 using Eq. 14 yielded membrane permeabilities for *p*-toluic acid and *p*-hydroxymethyl benzoic acid of  $1.1 \pm 0.2 \text{ cm s}^{-1}$  and  $(1.6 \pm 0.4) \times 10^{-3} \text{ cm s}^{-1}$ , respectively. These values and the permeability coefficient of acetamide are listed in Table 1 along with partition coefficients and ionization constants of these compounds.

As both substrates have similar molecular size and shape and therefore are likely to exhibit similar diffusion behavior, their relative ability to partition from water into the barrier domain in the bilayer becomes the major determinant of their relative permeabilities. If the transport barrier resides in a nonpolar hydrocarbon region, permeabilities should correlate well with the corresponding hexadecane/water partition coefficients listed in Table 1. The ratio of these two partition coefficients is  $8.35 \times 10^3$  corresponding to an incremental free energy change  $[\Delta(\Delta G^0)_{OH}]$  of 5.3 kcal/mole for the added  $-OH$  group. This value compares favorably with previously reported determinations of  $\Delta(\Delta G^0)_{OH}$ , the group contri-

bution to the free energy of transfer of an aliphatic hydroxyl substituent from water to hydrocarbon, which have ranged from 5.28 to 5.74 kcal/mol (35–37, 24). On the other hand, if the bilayer/water interface is rate-determining, group contributions to transport should reflect a more polar, hydrogen-bonding environment. On this basis, octanol might be expected to correlate with bilayer transport and, indeed, octanol has been suggested as a good model solvent for lipid bilayers (38–39). From the partition coefficients shown in Table 1, we estimate an  $-OH$  group contribution for solute transfer from water to octanol of 2.0 kcal/mol.

Values reported in the literature for the hydroxyl group contribution to the free energy of transfer from water to octanol vary from 1.6 kcal/mol estimated from the Hansch substituent constant for an aliphatic  $-OH$ ,  $\pi_{OH}$ , reported by Leo et al. (40), to a value of 2.9 kcal/mol estimated by Stein (24). Our value is nearer the low end of this rather broad range. The incorporation of a hydroxyl group into *p*-toluic acid decreases its membrane permeability coefficient by a factor of 700, corresponding to an  $-OH$  group contribution of 3.9 kcal/mol. To our knowledge, this is the first determination of the  $-OH$  group contribution obtained from a comparison of lipid bilayer permeabilities of two molecules which differ in a single hydroxyl group which is completely isolated from neighboring hydrogen bonding groups on the same molecule. In the past, for example, Orbach and Finkelstein (41) obtained a  $\Delta(\Delta G^0)_{OH}$  of only 2.3 kcal/mol from a comparison of the permeability coefficients of glycerol and 1,2-butanediol but pointed out that the hexadecane/water partition coefficient ratio for these compounds was also much lower than expected due, perhaps, to internal hydrogen bonding in glycerol. Diamond and Wright (42) obtained an  $-OH$  group contribution of 3.6 kcal/mol from the relative permeabilities of 1,6-hexanediol and 1,2,6-hexanetriol in *Nitella mucronata* (43) but again, intramolecular hydrogen-bonding may have diminished the effective hydrophobicity of the additional  $-OH$  in 1,2,6-hexanetriol. Our value (3.9 kcal/mol) suggests that the barrier microenvironment is more selective to polar, hydrogen bonding groups than is the hydrogen-bonding solvent octanol although somewhat less selective than expected for a pure hydrocarbon environment. The barrier domain appears to be located

within the bilayer interior, and not at the interface. An experimental probe of the polarity of the interfacial microenvironment is the  $-\text{OH}$  group contribution for equilibrium partitioning between water and lecithin liposomes, as solutes possessing one or more  $-\text{OH}$  groups probably localize near the interface in such a way that hydrogen bonding between the  $-\text{OH}$  and water or the polar head group of lecithin can occur. This  $-\text{OH}$  group contribution is 790–970 cal/mol (21), far smaller than the value obtained from permeabilities. These conclusions are qualitatively consistent with those of Stein (24) and Finkelstein et al. (2, 41) who have argued that the chemical selectivity of the permeability barrier within lipid bilayer membranes resembles a hydrocarbon solvent more closely than other more polar solvents.

This observation for a single functional group does not allow one to locate the barrier region precisely, but does appear to indicate that the barrier domain may reside within the ordered hydrocarbon chains where the effective local polarity may be slightly higher than in bulk alkane solvents. The local polarity of the ordered hydrocarbon domain may be influenced by its proximity to the interfacial region, by partial penetration of water molecules into the bilayer, or by the presence of double bonds in the chains. The role of double bonds may be assessed by examining hexadecene/water partition coefficients of our model permeants (shown in Table 1), from which an  $-\text{OH}$  group contribution of 4.6 kcal/mol, reduced from the value for the transfer from water to hydrocarbon, is calculated. Further reduction might be expected if water molecules can penetrate into lipid bilayers, as supported by both statistical mechanical analyses (44) and molecular dynamic simulations (45–46) which suggest that the penetration depth for water molecules into the bilayer interior is on the order of  $\sim 10$  Å.

In summary, these studies highlight the importance of considering the heterogeneity of lipid bilayer membranes in the development of a more fundamental and detailed understanding of transport across lipid bilayers. While Overton's rule assumes the bilayer to be a homogeneous phase and thus, predicts that transport rates should be inversely proportional to bilayer thickness, variation of the membrane thickness by varying the hydrocarbon content of the central, disordered region of planar lipid bilayers has been shown to have no effect on the permeability coefficient for acetamide. Further, we have validated a method for obtaining well isolated group contributions to the free energy of transfer of permeants into the permeability barrier domain. This method was used to obtain the  $-\text{OH}$  group contribution which provides additional evidence that the permeability barrier may be located in the more highly ordered, peripheral hydrocarbon regions of the bilayer. A more complete set of group contributions, currently being gen-

erated in our laboratories, will more definitively characterize the chemical nature of this barrier domain.

## APPENDIX

### A derivation of working equations for $C_m^*$

Because of the linear response of the potentiostat, the current going through the standard capacitor ( $I_0$ ) and the lipid membrane ( $I_m$ ) can be expressed as

$$I_0 = \frac{V_0}{Z_p} = \frac{V_i}{Z_0} \quad (\text{A.1})$$

and

$$I_m = \frac{V_m}{Z_p} = \frac{V_i}{Z_m}, \quad (\text{A.2})$$

where  $V_0$  and  $V_m$  are the output voltages from the potentiostat to the lock-in amplifier when the input potential  $V_i$  is applied to the standard capacitor and the lipid membrane, respectively, and  $Z_p$ ,  $Z_0$  and  $Z_m$  are, respectively, the impedances of the potentiostat, the standard capacitor and the lipid membrane.

The AC output to the lock-in amplifier can be expressed in terms of complex variables

$$V_0 = |A_0| \exp(i\phi_0) \quad (\text{A.3})$$

and

$$V_m = |A_m| \exp(i\phi_m), \quad (\text{A.4})$$

where  $(A_0, A_m)$  and  $(\phi_0, \phi_m)$  are the amplitudes and phase shifts observed for the standard capacitor and the membrane system.

Combining Equations (A.1)–(A.4) yields

$$Z_m^*/Z_0 = V_0/V_m = \left| \frac{A_0}{A_m} \right| \exp\{i(\phi_0 - \phi_m)\}. \quad (\text{A.5})$$

Writing  $Z_m$  and  $Z_0$  in terms of complex capacitances  $C_m^*$  and  $C_0$  one has

$$Z_0 = 1/2\pi f C_0 j \quad (\text{A.6})$$

and

$$Z_m^* = 1/2\pi f C_m^* j. \quad (\text{A.7})$$

Substituting Equations (A.6) and (A.7) into (A.5) and comparing with Eq. 1 gives the working equations in Eqs. 2 and 3.

This work was supported by a research grant from Glaxo, Inc. Instrumentation support was provided by a Biomedical Research Support Grant from the College of Pharmacy, University of Utah, and by a Faculty Research Grant from the University of Utah.

Received for publication 16 December 1991 and in final form 10 March 1992.

## REFERENCES

- McElhaney, R. N. 1975. Membrane lipid, not polarized water, is responsible for the semipermeable properties of living cells. *Biophys. J.* 15:777–784.

2. Finkelstein, A. 1976. Water and nonelectrolyte permeability of lipid bilayer membranes. *J. Gen. Physiol.* 68:127-135.
3. Sandermann, H. 1978. Regulation of membrane enzymes by lipids. *Biochim. Biophys. Acta.* 515:209-237.
4. Kimelberg, H. K. 1977. The influence of membrane fluidity on the activity of membrane-bound enzymes. *Cell Surf. Rev.* 3:205-298.
5. Mueller, P., D. O. Rudin, H. T. Tien, and W. C. Wescott. 1963. Methods for the formation of single bimolecular lipid membranes in aqueous solution. *J. Phys. Chem.* 67:534-535.
6. White, S. H. 1970. A study of lipid bilayer membrane stability using precise measurement of specific capacitance. *Biophys. J.* 10:1127-1148.
7. White, S. H., and T. E. Thompson. 1973. Capacitance, area, and thickness variations in thin lipid films. *Biochim. Biophys. Acta.* 323:7-22.
8. Montal, M., and P. Mueller. 1972. Formation of bimolecular membranes from lipid monolayers and a study of their electrical properties. *Proc. Natl. Acad. Sci. USA.* 69:3561-3566.
9. Anderson, J. S., and K. Saddington. 1949. The use of radioactive isotopes in the study of the diffusion of ions in solution. *J. Chem. Soc.* 1:381-386.
10. McIntosh, T. J., S. A. Simon, and R. C. MacDonald. 1980. The organization of *n*-alkanes in lipid bilayers. *Biochim. Biophys. Acta.* 597:445-463.
11. Pope, J. M., L. W. Walker, and D. Dubro. 1984. On the ordering of *n*-alkane and *n*-alcohol solutes in phospholipid bilayer model membrane systems. *Chem. Phys. Lipids.* 35:259-277.
12. Fettiplace, R., D. M. Andrews, and D. A. Haydon. 1971. The thickness, composition and structure of some lipid bilayer natural membranes. *J. Membr. Biol.* 5:277-296.
13. Seelig, J. 1977. Deuterium magnetic resonance: theory and application to lipid membranes. *Quart. Rev. Biophys.* 10:353-418.
14. White, S. H. 1978. Formation of "solvent-free" black lipid bilayer membrane from glyceryl monooleate dispersed in squalene. *Biophys. J.* 23:337-347.
15. Simon, S. A., L. J. Lis, R. C. MacDonald, and J. W. Kauffman. 1977. The noneffect of a large linear hydrocarbon, squalene, on the phosphatidylcholine packing structure. *Biophys. J.* 19:83-90.
16. Guggenheim, E. A. 1977. Thermodynamics. North-Holland, New York.
17. Small, D. M. 1967. Phase equilibria and structure of dry and hydrated egg lecithin. *J. Lipid Res.* 8:551-558.
18. Reiss-Husson, F. 1967. Structure des phases liquide-cristallines de differents phospholipides, monoglycerides, sphingolipides, anhydres on en presence d'eau. *J. Mol. Biol.* 25:363-382.
19. Lecuyer, H., and D. G. Dervichian. 1969. Structure of aqueous mixtures of lecithin and cholesterol. *J. Mol. Biol.* 45:39-57.
20. Michael, F. B., J. Seelig, and U. Haberland. 1979. Structural dynamics in phospholipid bilayers from deuterium spin-lattice relaxation time measurements. *J. Chem. Phys.* 70:5045-5053.
21. Diamond, J. M., and Y. Katz. 1974. Interpretation of nonelectrolyte partition coefficients between dimyristoyl lecithin and water. *J. Membr. Biol.* 17:121-154.
22. Gary, C. M., and H. W. Weber. 1969. Diffusion of alcohols and amides in water from 4 to 37°. *J. Phys. Chem.* 73:1155-1156.
23. White, S. H. 1972. Analysis of the torus surrounding planar lipid bilayer membranes. *Biophys. J.* 12:432-445.
24. Stein, W. D. 1986. Transport and Diffusion Across Cell Membranes. Academic Press, Inc.
25. Hayduk, W., and S. Ioakimidis, 1976. Liquid diffusivities in normal paraffin solvents. *J. Chem. Eng. Data.* 21:255-260.
26. De Young, L. R., and K. A. Dill. 1988. Solute partitioning into lipid bilayer membranes. *Biochemistry.* 27:5281-5289.
27. De Young, L. R., and K. A. Dill. 1990. Partitioning of nonpolar solutes into bilayers and amorphous *n*-alkanes. *J. Phys. Chem.* 94:801-809.
28. Marqusee, J. A., and K. A. Dill. 1986. Solute partition into chain molecule interphases: monolayers, bilayer membranes, and micelles. *J. Chem. Phys.* 85:434-444.
29. Walter, A., and J. Gutknecht. 1984. Monocarboxylic acid permeation through lipid bilayer membranes. *J. Membr. Biol.* 77:225-264.
30. Gutknecht, J., L. J. Bruner, and D. C. Tosteson. 1972. The permeability of thin lipid membranes to bromide and bromine. *J. Gen. Physiol.* 59:486-502.
31. Gutknecht, J., and D. C. Tosteson. 1973. Diffusion of weak acids across lipid bilayer membranes: effects of chemical reactions in the unstirred layers. *Science (Wash. DC).* 182:1258-1261.
32. Robinson, R. A., and R. H. Stokes. 1959. Electrolyte Solutions. Butterworths, London.
33. Weast, R. C. editor. 1981-1982. Handbook of Chemistry and Physics. 62nd Edition. CRC Press, Inc., Boca Raton, FL.
34. Deleted in proof.
35. Pescar, R. E., and J. J. Martin. 1966. Solution thermodynamics from gas-liquid chromatography. *Anal. Chem.* 38:1661-1669.
36. Martire, D. E., and P. Riedl. 1968. A thermodynamic study of hydrogen bonding by means of gas-liquid chromatography. *J. Phys. Chem.* 72:3478-3488.
37. Rytting, J. H., L. P. Huston, and T. Higuchi. 1978. Thermodynamic group contributions for hydroxyl, amino, and methylene groups. *J. Pharm. Sci.* 67:615-618.
38. Wolosin, J. M., and H. Ginsburg. 1975. The permeation of organic acids through lecithin bilayers: resemblance to diffusion in polymers. *Biochim. Biophys. Acta.* 389:20-33.
39. Wolosin, J. M., H. Ginsburg, W. R. Lieb, and W. D. Stein. 1978. Diffusion within egg lecithin bilayers resembles that within soft polymers. *J. Gen. Physiol.* 71:93-100.
40. Leo, A., C. Hansch, and D. Elkins. 1971. Partition coefficients and their uses. *Chem. Rev.* 71:525-616.
41. Orbach, E., and A. Finkelstein. 1980. The nonelectrolyte permeability of planar lipid bilayer membranes. *J. Gen. Physiol.* 75:427-436.
42. Diamond, J. M., and E. M. Wright. 1969. Biological membranes: the physical basis of ion and non-electrolyte selectivity. *Annu. Rev. Physiol.* 31:581-646.
43. Collander, R. 1954. The permeability of Nitella cells to non-electrolytes. *Physiol. Plantarum.* 7:420-445.
44. Leermakers, F. A. M., J. M. H. M. Scheutjens, and J. Lyklema. 1983. On the statistical thermodynamics of membrane formation. *Biophys. Chem.* 18:535-560.
45. Egberts, E., and H. J. C. Berendsen. 1988. Molecular dynamics simulation of a smectic liquid crystal with atomic detail. *J. Chem. Phys.* 89:3718-3732.
46. Nicklas, K., J. Bocker, M. Schlenkrich, J. Brickmann, and P. Bopp. 1991. Molecular dynamics studies of the interface between a model membrane and an aqueous solution. *Biophys. J.* 60:261-272.